Effects of Pulmonary Vascular Obstruction on Right Ventricular Afterload[1-3]

JAMES M. FITZPATRICK[4] and BRYDON J. B. GRANT[5]

SUMMARY We compared the effects of three forms of vascular obstruction: positive end-expiratory pressure (PEEP), ensnarement of the left main pulmonary artery (SN), and pulmonary thromboembolism (EMB) on right ventricular afterload. We measured right ventricular and pulmonary arterial pressures and flow in open-chested dogs under anesthesia (n = 8). Pulmonary artery input impedance (Z_{in}) was calculated by Fourier analysis of the pressure and flow waves. Characteristic impedance (Z_c) and pulmonary arterial compliance (C_a) were estimated from Z_{in} with a lumped parameter model. Although PEEP, SN, and EMB all increased mean pulmonary arterial pressure, PEEP, had negligible effect on Z_c and C_a, whereas SN increased Z_c but decreased C_a (+24% and −49%, respectively), and EMB decreased both Z_c and C_a (−33% and −39%, respectively). These changes of Z_c affect wave reflection and alter the energy transmission ratio, which is the ratio of hydraulic power output in the measured and forward waves ($\dot{W}_m/\dot{W}_f$). Under control conditions, $\dot{W}_m/\dot{W}_f$ was 62% and was not affected significantly by SN (59%) or by PEEP (46%), but it fell significantly to 30% after EMB. Simulation of these experiments in a mathematical model suggested that the increase of Z_c with SN was due to an active neurohumoral effect; all other responses were consistent with passive mechanical effects. In additional experiments, we tested the effects of meclofenamate (n = 6) and ketanserin (n = 6) and of atropine and vagotomy (n = 5) on the response to SN and EMB. The serotonin antagonist, ketanserin, blunted the increase of Z_c to SN, but none of the interventions significantly affected the response of Z_c or C_a to EMB. We conclude that SN has different effects on right ventricular afterload than does EMB. SN appears to involve an active neurohumoral mechanism that is attenuated by ketanserin and acts to reduce the adverse effects of wave reflection.

AM REV RESPIR DIS 1990; 141:944-952

Introduction

Pulmonary thromboembolism is one of the major causes of hospital morbidity and mortality. About 50,000 deaths occur annually as a result of this condition. The primary event that leads to these deaths is an acute increase in right ventricular afterload leading to cor pulmonale (1). In an effort to understand this process more clearly, we studied the effects of pulmonary thromboembolism on afterload by measuring pulmonary artery input impedance (Z_{in}). The estimation of impedance provides a more complete description of the right ventricular afterload than does the estimation of resistance since it takes into account the opposition to both steady and pulsatile flow (2). Resistance only describes the opposition to steady or mean flow. The oscillatory components of pressure and flow are important because approximately 30 to 48% of the total hydraulic power is contained in the pulsatile component of blood flow in the main pulmonary artery (3).

The pattern of the pressure and flow waves measured in the main pulmonary artery represent the result of a collision between a forward wave from the heart with a backward wave reflected from the more peripheral parts of the pulmonary arterial tree. Characteristic impedance (Z_c) is the input impedance in the absence of wave reflection and is dependent primarily on the mechanical properties of the main pulmonary artery. Direct measurement of Z_c is problematic because wave reflection is always present in the intact system, but at high frequencies, Z_{in} approximates Z_c. Wave reflection has a detrimental effect by causing a phase shift between pressure and flow waves that reduces the hydraulic power output of the right ventricle delivered into the main pulmonary artery.

We compared the changes induced in input impedance with vascular obstruction caused by embolism with autologous clot (EMB) with two other forms of obstruction: positive end-expiratory pressure (PEEP), which results in compression of the alveolar vessels, and ensnarement of the left main pulmonary artery (SN). PEEP causes obstruction at a microvascular level and a snare causes large vessel obstruction. EMB obstructs pulmonary arteries between these extremes. We used two approaches to determine whether the observed responses were due to active neurohumoral mechanisms or to passive mechanical factors as a result of the increase in pulmonary artery pressure produced by obstruction. First, the experimental results were compared with the results obtained from a mathematical model of the canine pulmonary circulation. The mathematical model describes changes that would be anticipated from passive mechanical effects alone. A discrepancy between results obtained by the experimental and mathematical model would suggest an active neurohumoral effect may be operating. Second, we determined if the pulmonary hemodynamic response was altered by the cyclooxygenase inhibitor, meclofenamate, by the serotonin antagonist, ketanserin, or by the combination of atropine and vagotomy.

Methods

Animal Preparation

Experiments were performed on 25 mongrel dogs weighing between 17 and 21 kg. Anesthesia was induced with thiamylal 1.5 mg·kg^{-1}

(Received in original form January 10, 1989 and in revised form September 15, 1989)

[1] From the Department of Medicine, State University of New York at Buffalo, Buffalo, New York.

[2] Supported by a grant from the Whitaker Foundation and by Grant HL-41011 from the National Institutes of Health.

[3] Correspondence and requests for reprints should be addressed to B. J. B. Grant, M.D., Erie County Medical Center (Pulmonary Division), 462 Grider Street, Buffalo, NY 14215.

[4] Recipient of a Research Fellowship Award from the American Lung Association.

[5] Recipient of Research Career Development Award HL-01418 from the National Institutes of Health.

and maintained with a bolus injection of alpha chloralose (120 mg·kg^{-1}) followed by a continuous infusion of 43 mg·kg^{-1}·h^{-1}. The dogs were intubated and ventilated with a Harvard model 681 volume cycled ventilator (Harvard Apparatus Co., South Natick, MA). Intravenous pancuronium bromide (0.1 mg·kg^{-1}) was used for muscular paralysis. A catheter was placed in the right femoral artery for monitoring of systemic arterial pressure with a Statham P23 ID pressure transducer (Statham Instruments, Oxnard, CA). Airway pressure was monitored with a Validyne differential pressure transducer (Validyne Corp., Northridge, CA).

The pulmonary trunk was exposed via a left thoracotomy in the fifth intercostal space. PEEP (5 cm H_2O) was applied to prevent atelectasis. This amount of PEEP was considered as the control level. A Statham electromagnetic flow probe (internal diameter between 16 and 18 mm) was placed around the main pulmonary artery. Two 3F micromanometer-tipped catheters (Millar, Houston, TX) were inserted into the right ventricle and the main pulmonary artery through stab wounds on the right ventricular outflow tract. All pressures were zeroed relative to atmosphere.

Pulmonary Vascular Obstruction

Three methods were used to produce pulmonary vascular obstruction: PEEP, SN, and EMB. PEEP was administered at 15 cm H_2O for 5 min. The left main pulmonary artery was totally occluded by tightening a snare around the vessel approximately 1 to 2 cm distal to the bifurcation for 3 min. Emboli were made from 20 to 30 ml of autologous blood. Thrombi were formed either spontaneously in a glass beaker or by the addition of 100 NIH units of thrombin (Sigma Chemical, St. Louis, MO) to the blood. The clots were placed into a syringe with a wide-bore nozzle 5 mm in internal diameter and injected through a large venous catheter (at least 5 mm in internal diameter).

Experimental Protocol

In the first series of experiments on eight dogs, control measurements at 5 cm H_2O PEEP were taken between each perturbation. Hemodynamic measurements were made in the following order of experimental conditions: control, PEEP, control, SN, control, EMB. We made measurements immediately after administration of the clots and at 10 and 20 min later unless there was hemodynamic instability during the 45-s period required for data acquisition.

The second series of experiments was conducted in 17 dogs to test the effects of one of three interventions: meclofenamate (3 mg·kg^{-1} intravenously) in six dogs, ketanserin (0.15 mg·kg^{-1} intravenously) in six dogs, or atropine (0.1 mg·kg^{-1} intravenously) and bilateral cervical vagotomy in five dogs. In each group of dogs, measurements were made in the following order of experimental conditions: control, PEEP, control, SN, control followed by the intervention. We allowed 30 min after meclofenamate administration, 10 min after ketanserin, and 10 min after atropine and vagotomy before data collection. Measurements were then obtained in the following order of experimental conditions: control, PEEP, control, SN, control, and EMB. Hereafter, the term "vagotomy" will be used to indicate the combination of atropine administration and bilateral cervical vagotomy.

Data Collection and Analysis

All analog signals were displayed on an eight-channel Gould 2800S recorder (Gould Instruments, Cleveland, OH). These analog signals were converted to digital form (Data Translation DT2801A) with an AT compatible computer (Wells-American A Star, Columbia, SC). The pressure and flow waves were sampled at 500 Hz. Single cardiac cycles at end expiration from 10 successive breaths were used for Fourier analysis as described previously (4).

Estimation of Characteristic Impedance and Pulmonary Arterial Compliance

We used a lumped parameter model in order to calculate characteristic impedance and pulmonary arterial compliance (4). An electrical representation of the lumped parameter model is shown in figure 1. The resistor R_{in} represents input resistance (mean pressure divided by mean flow). The resistor Z_c represents characteristic impedance, which depends primarily on the inertance and compliance per unit length of the main pulmonary artery. The capacitor C_a represents pulmonary arterial compliance. The value of the inductance (L) is zero or close to zero, but it can improve significantly the ability of the model to fit the experimental data (4). Its values are not reported here because they are close to zero and are not known to be of any physiologic significance. Input impedance is calculated by Fourier analysis of the pressure and flow waves. The four elements of the model can then be simultaneously estimated by approximating the impedance of lumped parameter model to the measured pulmonary arterial input impedance spectra. The input impedance of the network was calculated and compared with the experimentally measured impedance with the maximal likelihood criterion (4). Parameter values were varied by an iterative method to obtain the best fit of model impedance to the measured impedance.

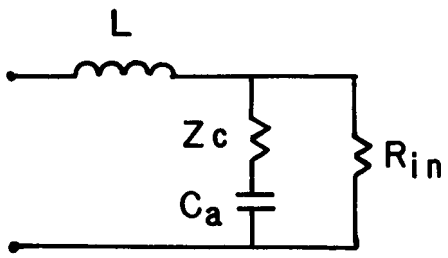

Fig. 1. An electrical representation of the lumped parameter model. R_{in} is the input resistance, C_a is the pulmonary arterial compliance, Z_c is the characteristic impedance and L is inductance.

Calculation of Power

Hydraulic power has two components: one caused by the steady or mean level of pressure and flow, the other caused by their oscillatory components. Each component is the summation of three parts: pressure, gravitational, and kinetic power. The largest quantity is pressure power, which is calculated from the product of pressure and flow. Gravitational forces are negligible, but the amount of kinetic energy, although small, is taken into account. We used the equations described by Milnor and coworkers (3) to calculate the components of hydraulic power, but we used a time domain method to determine the oscillatory component of pressure power.

The total or measured pressure and flow waves are resolved into their forward and backward or reflected waves with equations derived by Westerhof and coworkers (5). The equations for calculating the forward waves are as follows:

$$P_f(j) = 0.5\,[P_m(j) + Z_c\dot{Q}_m(j)] \quad (1)$$

$$\dot{Q}_f(j) = P_f(j)/Z_c \quad (2)$$

where P(j) and $\dot{Q}$(j) are the instantaneous pressure and flow at data point j. Each data point is the ensemble average of single cardiac cycles at end expiration from 10 successive breaths. Subscripts m and f refer to the measured and forward values, respectively.

The forward component of hydraulic power ($\dot{W}_f$) was calculated from the forward pressure and flow waves. The ratio of measured power to forward power ($\dot{W}_m/\dot{W}_f$) is the energy transmission ratio (6). It expresses the proportion of forward wave power that is measured in the main pulmonary artery and assesses the effect of wave reflection on reducing the hydraulic power output.

Mathematical Model

To simulate these experiments, we used a mathematical model of the canine pulmonary vasculature similar to that developed by Wiener and colleagues (7) and Milnor (8). Details of this analysis are provided in *Appendix 1.* The essential features of the model are as follows. First, pressure-flow relations follow the fifth power law as proposed by Zhuang and coworkers (9). Second, alveolar pressure is assumed to be the extravascular pressure for vessels less than 100 μm in diameter. Third, there are 43 vascular generations from the main pulmonary artery (Generation 1) to the left atrium.

The snare was simulated by halving the number of branches for Generations 2 to 43. Embolism was simulated by halving the number of branches for Generations 8 to 43. The arteries of Generation 8 are less than 5 mm in internal diameter, which is the approximate inner diameter of the catheter through which

the clots were injected. Left atrial pressure was assumed to be constant at 4 cm H_2O. The input variables are the measured pulmonary arterial flow ($\dot{Q}$) and alveolar pressure, which is assumed equal to airway pressure at end expiration. The output variables are pulmonary arterial pressure, Z_c and C_a.

Statistical Analysis

In the first series of experiments, we used an analysis of variance for a two-way experimental design and Scheffe's method to determine differences between the means of each physiologic variable (10).

In the second series of experiments, we used a factorial analysis of variance for each of the three groups of dogs to determine the effect of SN, the effect of the intervention per se, and the effect of the intervention on the hemodynamic response to SN. We used analysis of variance for repeated measures to determine the effect of the intervention on the hemodynamic response to EMB (10). We compared the effect of EMB measured in the first series of experiments with the effects of EMB measured after each of the three interventions. In all cases, significance was accepted at the 5% level.

Results

Control values of systemic arterial blood pressure, heart rate, mean pulmonary artery pressure (Ppa), mean $\dot{Q}$, Z_c, and C_a did not change significantly during the course of the experiment. This finding indicates that the observed changes were due to the various forms of administered obstruction and not to deterioration of the experimental preparation.

Both the experimental and mathematical model data for mean Ppa, mean $\dot{Q}$, Z_c, and C_a, respectively, are displayed in figure 2. The model estimates changes that result from passive mechanical factors. The increase in mean Ppa with EMB was predicted correctly. The model slightly underestimated the effect of PEEP, but grossly overestimated the increase of mean Ppa with SN. The values of mean $\dot{Q}$ were used as inputs for the mathematical model. The changes of pulmonary arterial compliance were predicted correctly by the model for PEEP, SN, and EMB. The model also predicted the changes of Z_c caused by PEEP, but underestimated the decrease of Z_c with EMB. The greatest discrepancy between the experimental and model results was the change of Z_c after SN. There was a marked increase in Z_c with respect to control, but the model predicted a small change in the opposite direction.

To determine if this increase of characteristic impedance was a spurious result of our lumped parameter model, we calculated characteristic impedance by the more unusual approaches of averaging the moduli of pulmonary input impedance (11–15). Similar results were obtained in four of the five methods used (see *Appendix 2*).

Pulmonary arterial pulse pressure (PP) decreased with EMB, but SN caused PP to increase (table 1). The increased PP resulted from an increase in systolic but no change in diastolic pulmonary arterial pressures for SN. In addition, PEEP and EMB increased right ventricular end-diastolic pressure and heart rate, and decreased systemic arterial blood pressure. None of these changes occurred with SN.

The effect of wave reflection on both the measured pressure and flow waves is illustrated in figure 3. The forward and reflected pressure waves summate to produce the measured pressure wave. However, the measured flow wave is the difference between the forward and reflected waves because the reflected wave travels in the opposite direction to the forward wave. There are relatively small differences between the forward and measured waves under control conditions and with SN. This difference increased with PEEP and was even more pronounced with EMB, which indicated a substantial effect of wave reflection. The influence of wave reflection on pulmonary hemodynamics was assessed from its effect on hydraulic power in the main pulmonary artery.

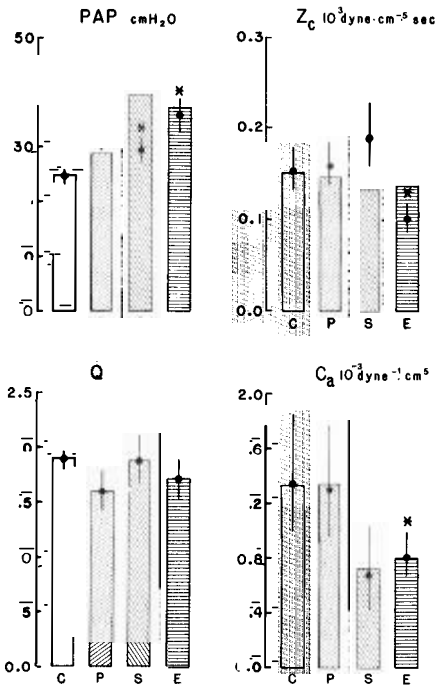

Fig. 2. Effects of pulmonary vascular obstruction on hemodynamics: theoretical and experimental results. Experimental data are shown as solid circles ± 2 SEM. Data from the mathematical model calculated from control measurements are shown as open bars. Mean pulmonary arterial pressure (PAP, *upper left panel*), characteristic impedance (Z_c, *upper right panel*), and pulmonary arterial compliance (C_a, *lower right panel*) are output variables of the model. The measured values of pulmonary arterial flow ($\dot{Q}$, *lower left panel*) were used as input values for the model. Data under four conditions are shown: control (C), PEEP (P), ensnarement (S), and embolism (E). Z_c and C_a were analyzed with a logarithmic transformation. The asterisks represent statistically significant ($p < 0.05$) differences from control values.

Hydraulic Power

The changes of right ventricular power output in response to the three types of vascular obstruction are displayed in figure 4. Total measured wave power ($\dot{W}_m$) was not changed statistically by any of the three forms of obstruction. There was no significant relation between heart rate and $\dot{W}_m$. There were, however, significant differences in the hydraulic power contained in the pulsatile components of the measured pressures and flow waves ($\dot{W}_m$osc): $\dot{W}_m$osc increased with SN but decreased with PEEP and EMB. Although $\dot{W}_m$osc varies inversely with heart rate ($p < 0.001$), there was no significant relation between heart rate and the hydraulic power in the oscillatory

TABLE 1

EFFECT OF PULMONARY VASCULAR OBSTRUCTION ON HEMODYNAMIC VARIABLES*

Variable	Control	PEEP	SN	EMB	p Value
PP, cm H_2O	0.7)	19.3 (1.9)	27.9* (2.8)	18.9* (0.7)	< 0.005
PpaS, cm H_2O	1.4)	40.7 (1.5)	46.1* (3.1)	46.3* (3.1)	< 0.005
PpaD, cm H_2O	0.6)	21.5* (0.8)	18.2 (2.1)	28.6* (1.8)	< 0.005
RVEDP, cm H_2O	0.7)	10.5* (1.5)	8.9 (1.2)	10.3* (1.4)	< 0.005
HR, beats/min	9.6)	155.3* (7.0)	129.0 (9.5)	140.3* (5.4)	< 0.005
BP, mm Hg	5.5)	113.0* (9.3)	130.7 (6.4)	109.9* (11.0)	< 0.01

Definition of abbreviations: PEEP = positive end-expiratory pressure; SN = ensnarement of the left main pulmonary artery; EMP = embolism; PP = pulmonary arterial pulse pressure; PpaS and PpaD = systolic and diastolic pulmonary arterial pressures, respectively; RVEDP = right ventricular end-diastolic pressure; HR = heart rate; BP = mean systemic arterial blood pressure.

* 1 SEM is given in parentheses. The p value is the probability of difference between the four conditions. The asterisk indicates a significant difference from control value.

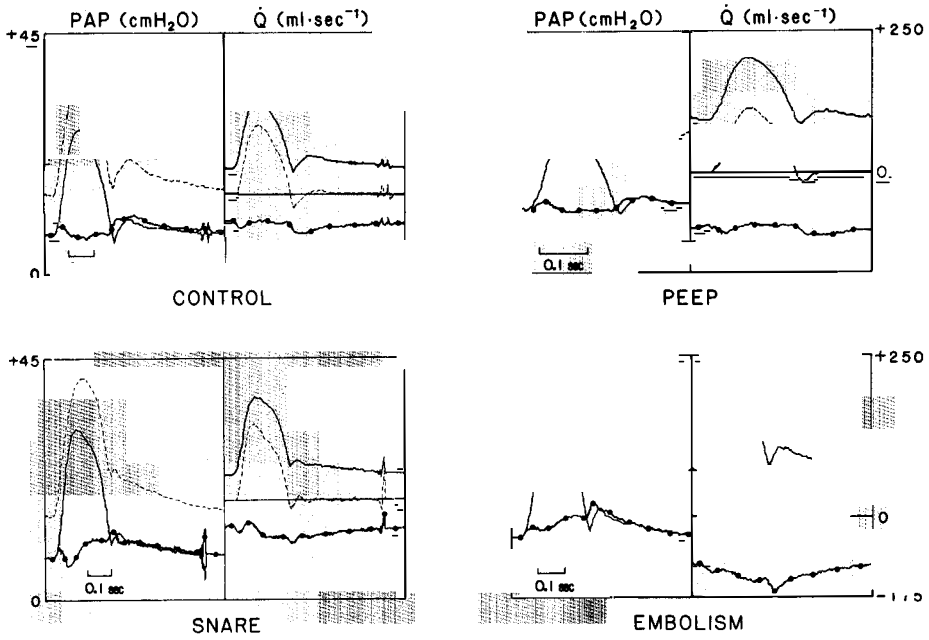

Fig. 3. An example of the effects of wave reflection on the pulmonary artery pressure and flow waves from one experiment. For each condition, pressure waves are shown in the left panel and flow waves in the right panel. The solid line represents the forward pressure and flow waves. The dashed lines are the measured pressure and flow waves. The continuous lines with dots are the reflected pressure and flow waves.

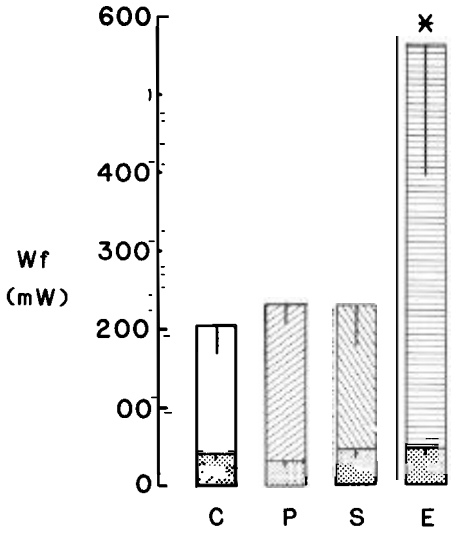

Fig. 5. Effect of pulmonary vascular obstruction on the hydraulic power in the forward wave. The bars represent the total hydraulic power (expressed in milliwatts on the ordinate) in the forward wave ($\dot{W}_f$) under four conditions: control (C), increased positive end-expiratory pressure (P), with a snare (S), and after embolism (E). The dotted areas indicate the hydraulic power contained in the pulsatile terms ($\dot{W}_f$osc). The error bars represent 1 SEM. There was a significant difference among conditions ($p < 0.025$) for total $\dot{W}_f$, but no significant difference for W_f contained in the pulsatile terms. The asterisk indicates a significant difference from control value.

component of the forward wave (figure 5). The most striking finding was the dramatic rise in the total forward wave power ($\dot{W}_f$) with EMB, which increased to 277% of control levels. The changes caused by PEEP and SN were not significant. The effect of wave reflection on the energy transmission ratio ($\dot{W}_m/\dot{W}_f$) are shown in figure 6. This ratio was reduced by PEEP and EMB, but only the reduction with EMB attained statistical significance. There was no significant relation between $\dot{W}_m/\dot{W}_f$ and heart rate.

The proportion of total measured hydraulic power in the pulsatile components ($\dot{W}_m$osc/$\dot{W}_m$) is related directly to the amount of wave reflection (as judged by the ratio $\dot{W}_m/\dot{W}_f$) regardless of the form of pulmonary vascular obstruction (figure 7). Therefore, wave reflection appears to be responsible for the reduction of hydraulic power in the pulsatile components of pressure and flow.

Effects of Meclofenamate, Ketanserin, and Vagotomy

The effects of meclofenamate, vagotomy, and ketanserin on the mean Ppa, mean $\dot{Q}$, Z_c, and C_a in response to ensnarement are shown in table 2. The results of the statistical analysis are shown in table 3. As in the first series of experiments, SN caused an increase in mean Ppa and Z_c, no change in mean $\dot{Q}$, and a decrease in C_a. Meclofenamate, vagotomy, and ketanserin had no significant effect on mean Ppa, $\dot{Q}$, Z_c, or C_a except for a small but significant increase in mean Ppa and mean $\dot{Q}$ after vagotomy. The only intervention that significantly affected the hemodynamic response to ensnarement was ketanserin, which significantly reduced the increase of Z_c with ensnarement.

The pulmonary vascular responses to embolism in four groups of dogs are com-

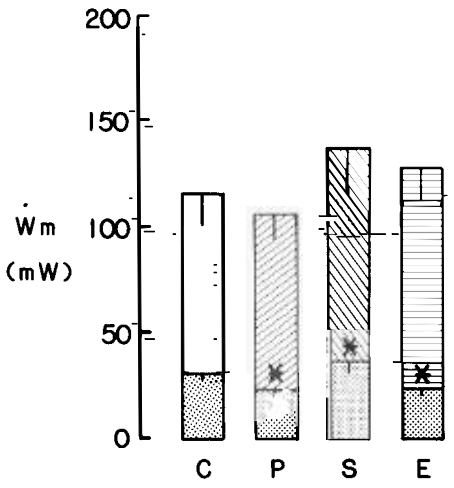

Fig 4. Effect of pulmonary vascular obstruction on the hydraulic power in the measured wave. The bars represent the total hydraulic power (expressed in milliwatts on the ordinate) in the measured wave ($\dot{W}_m$) under four conditions: control (C), increased positive end-expiratory pressure (P), with a snare (S), and after embolism (E). The dotted areas indicate the hydraulic power contained in the pulsatile terms ($\dot{W}_m$osc). The error bars represent 1 SEM. There was a significant difference between conditions ($p < 0.025$) for hydraulic power contained in the pulsatile terms, but no significant difference among conditions for total hydraulic power. The asterisks indicate statistically significant differences from control values. One milliwatt is equivalent to 0.443 mm Hg·L·min^{-1}.

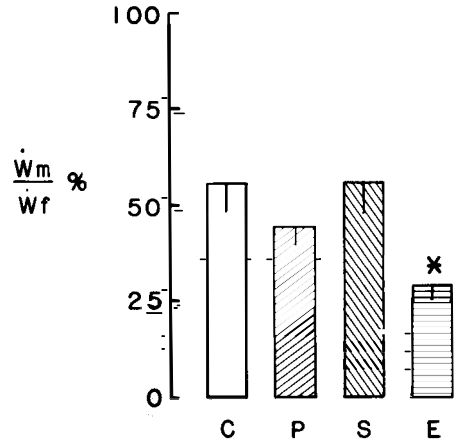

Fig. 6. Effects of pulmonary vascular obstruction on the energy transmission ratio. This bar chart shows the ratio of the measured hydraulic power to the forward hydraulic power ($\dot{W}_m/\dot{W}_f$) expressed as a percentage (ordinate) under four conditions: control (C), increased positive end-expiratory pressure (P), with a snare (S), and after embolism (E). The error bars represent 1 SEM. There was a significant difference between conditions ($p < 0.005$). The asterisk indicates a significant difference from control.

TABLE 4

EFFECT OF PRETREATMENT WITH MECLOFENAMATE AND KETANSERIN AND OF VAGOTOMY ON THE PULMONARY VASCULAR RESPONSE TO PULMONARY THROMBOEMBOLISM*

Pretreatment	EMB	Ppa ($cm\ H_2O$)	$\dot{Q}$ ($L \cdot min^{-1}$)	Z_c ($10^3\ dyne \cdot cm^{-5}\ s$)	C_a ($10^{-3}\ cm^5 \cdot dyne^{-1}$)
None, n = 8	B	24.9 ± 1.3	1.8 ± 0.2	0.16 $^{+0.03}_{-0.02}$	1.18 $^{+0.44}_{-0.32}$
	A	37.6 ± 3.4	1.7 ± 0.2	0.11 $^{+0.02}_{-0.02}$	0.73 $^{+0.15}_{-0.13}$
Meclofenamate, n = 6	B	25.0 ± 2.1	1.9 ± 0.4	0.16 $^{+0.08}_{-0.04}$	1.03 $^{+0.86}_{-0.46}$
		41.9 ± 5.6	1.7 ± 0.7	0.08 $^{+0.04}_{-0.03}$	0.61 $^{+0.06}_{-0.06}$
Vagotomy, n = 5	B	32.6 ± 1.7	1.9 ± 0.2	0.18 $^{+0.03}_{-0.02}$	0.92 $^{+0.33}_{-0.24}$
	A	55.1 ± 2.4	1.8 ± 0.2	0.10 $^{+0.03}_{-0.02}$	0.69 $^{+0.22}_{-0.17}$
Ketanserin, n = 6	B	25.8 ± 2.6	2.0 ± 0.2	0.15 $^{+0.01}_{-0.01}$	2.43 $^{+2.15}_{-1.14}$
	A	43.2 ± 6.0	1.4 ± 0.1	0.11 $^{+0.02}_{-0.01}$	0.65 $^{+0.34}_{-0.22}$
Effect of		Results of Repeated Measures Analysis of Variance (p values)			
Embolism		< 0.0001	0.035	0.0006	0.01
Pretreatment		< 0.05	NS	NS	NS
Interaction		NS	NS	NS	NS

For definition of abbreviations, *see* table 3.

* Data are expressed as mean ± 1 SEM. Logarithmic transformations of Z_c and C_a were used for statistical analysis. Measurements obtained before (B) and after (A) thromboembolism. Interaction term indicates the effect of pretreatment on the response to embolism.

for any unit change in transmural pressure (dS/dP), the equation can be modified with substitution to yield:

$$Z_c = [\rho/(\pi r^2 \cdot dS/dP)]^{0.5} \quad (4)$$

The discrepancy between the model and the experimental results implies that some active mechanism increased Z_c by a reduction in the compliance per unit length of the main pulmonary artery (dS/dP) and/or a decrease of vessel radius (r), probably because of an increase of smooth muscle tone in the main pulmonary artery.

The decrease in Z_c that occurred with embolism also occurred in the mathematical model. Therefore, this change can be attributed mainly to passive distention of the proximal pulmonary artery, although the extent of the decrease was larger than predicted. Although this passive mechanism explains most of the change of Z_c with thromboembolism, it does not exclude the possibility that active neurohumoral mechanisms are contributing to the observed response. The mathematical model predicted correctly the reduction of C_a with SN and EMB. This change is consistent with a reduction in the number of perfused vascular units induced by these modes of obstruction.

We used three interventions to determine the role of neurohumoral mechanisms: the administration of the serotonin antagonist ketanserin, meclofenamate, and vagotomy. Serotonin (16, 17) and cyclooxygenase products (18) have been implicated as contributing to the increased pulmonary vascular resistance in acute pulmonary embolism. Although the role of neural reflexes in acute pulmonary embolism has not been defined, we tested the effects of vagotomy because pulmonary baroreceptors in the dog are known to be stimulated by increases in Ppa (19). Our conclusion that the pulmonary hemodynamic response to SN is an active mechanism was confirmed by the fact that ketanserin blocked the increase in Z_c. Presumably, this effect is due to blocking 5-hydroxytryptamine$_2$ receptors although an alpha-1 adrenergic blocking effect of ketanserin cannot be excluded (20). The mechanism whereby ensnarement of the left main pulmonary artery releases serotonin is unclear. Serotonin may be released from platelets when the snare is applied, but it is difficult to conceive of how this humoral agent could exert its effect on the main pulmonary artery, which is upstream of the site at which the left main pulmonary artery was snared. There are several possible explanations. First, the local effects of serotonin may be propagated upstream through the smooth muscle, but this mechanism has been reported previously only in the peripheral systemic circulation (21). Second, this response may be conducted through the neural plexus and stimulating sympathetic nerves to release serotonin as an alternative neurotransmitter (22). This mechanism has been established previously only in the systemic circulation. Third, the humoral effects of SN may have reached the vaso vasorum of the main pulmonary artery through the bronchial circulation. However, it is likely that the serotonin would be cleared by the pulmonary circulation before reaching the systemic circulation. The present experiments do not distinguish between any of these possibilities.

Comparison of Our Results with Those of Others

In order to express the changes of input impedance in a more concise form, we used a lumped parameter model to estimate simultaneously input resistance, total pulmonary arterial compliance, and characteristic impedance. Our results for Z_c were comparable to values obtained in previous studies done in dogs of comparable size (15). Also, our measurements of C_a were similar to the results of Van den Bos and colleagues (23). To our knowledge, there have been no previous measurements of C_a in response to PEEP, SN, or EMB. However, there have been several measurements of Z_c in response to PEEP and SN.

Both Bergel and Milnor (24) and Calvin and coworkers (25) found no change in Z_c with PEEP; our results concur. Calvin and coworkers found that constriction of the main pulmonary artery increased Z_c. This result would be anticipated from equation 4 because of the reduction of the caliber of the main pulmonary artery. Our snare was placed around the left main pulmonary artery with care taken to avoid any distortion of the main pulmonary artery. This experiment has been conducted previously by Pouleur and colleagues (26), who found a similar increase of Z_c but interpreted this result differently. These investigators presumed that the reduction in cross-sectional area of the proximal pulmonary arterial tree would increase characteristic impedance; our mathematical model predicts otherwise, which leads us to conclude that this response is due to an active neurohumoral mechanism. The fact that we were able subsequently to

block this response supports this argument. This conclusion is in general agreement with that of Aramendia and coworkers (27). These investigators found that balloon occlusion of the left main pulmonary artery resulted in an increase in Ppa that could be blocked by local infiltration with lidocaine at the site of occlusion but not by atropine or vagotomy.

Hemodynamic Consequences

We assessed the hemodynamic consequences of changes in right ventricular afterload with various forms of vascular obstruction in terms of hydraulic power. Measured power was not affected significantly by PEEP, SN, or EMB (figure 4). The fact that we did not find a relation between heart rate and $\dot{W}_m$, which has been reported by Milnor and coworkers (3) is probably a reflection of the moderate changes in heart rate in our preparation. Despite the lack of statistical differences in $\dot{W}_m$ with pulmonary vascular obstruction, right ventricular end-diastolic pressure increased significantly with PEEP and EMB, but not with SN. It is difficult to determine from these experiments whether this increase in pressure results from differences in the right ventricular afterload or is due to differences of right ventricular function because systemic arterial blood pressure fell with PEEP and EMB but not with SN, which may have compromised coronary arterial perfusion.

The PEEP and SN, as shown in figure 5, had no significant effect on the total hydraulic power in the forward wave. But there was a dramatic 300% increase in the forward wave power after EMB. As a result, the energy transmission ratio ($\dot{W}_m/\dot{W}_f$) nearly halved with EMB (falling from 58 to 30%), whereas there were no significant effects of PEEP and SN (figure 6).

A decrease in the measured hydraulic power after EMB was avoided by a compensatory increase in the hydraulic power of the forward wave. These results illustrate the adverse effects of wave reflection on hydraulic power. The reduction in hydraulic power occurs because of the differing effects of the wave reflection on pressure and flow. For pressure, the reflected and the forward waves summate to form the measured pressure wave. For flow, the reflected wave subtracts from the forward wave to form the measured flow wave. Therefore, wave reflection causes the pressure and flow waves to become out of phase with each other. As a result, there is a decrease in hydraulic power because it is heavily dependent on the instantaneous product of pressure and flow. As wave reflection increases, as judged by a decrease of $\dot{W}_m/\dot{W}_f$, there is a decrease in the proportion of hydraulic power contained in the oscillatory components of the pulmonary circulation (figure 7).

These experiments demonstrate that wave reflection plays an important role in the hemodynamic effects of pulmonary embolism. The hemodynamic consequences of pulmonary hypertension depend on the cause of the pulmonary vascular obstruction. These experiments show that ensnarement of the main pulmonary trunk is not an adequate simulation of the right ventricular afterload that occurs after pulmonary thromboembolism (28). It seems unfortunate that the increase in Z_c with SN, which reduces wave reflection, does not occur with EMB. From a clinical standpoint, the primary goal should be to remove the cause of the increased wave reflection. The increased wave reflection with EMB is probably generated by waves impinging on fragments of the clots lying in the pulmonary arterial tree. This problem may be alleviated by fragmentation of the emboli into more peripheral parts of the pulmonary arterial tree, or by lysis of the thrombi. However, it takes time for these processes to take effect. Administration of vasoactive drugs immediately after pulmonary thromboembolism may have a beneficial effect by selectively stiffening the proximal pulmonary arteries. This action would have minimal effects on resistance but would increase characteristic impedance and reduce wave reflection.

In conclusion, we have shown that PEEP, SN, and EMB increase mean Ppa but have differing effects on Z_c and C_a. The changes of Z_c and C_a caused by PEEP and EMB result largely from passive mechanical effects. The increase of Z_c caused by SN, however, seemed to result from an active mechanism; this idea was confirmed by the finding that ketanserin attenuated this response. The effect of these changes on wave reflection was evaluated in terms of hydraulic power in the main pulmonary artery. We conclude that the changes of Z_c with SN minimizes wave reflection, but the changes of Z_c with EMB magnify the deleterious effects of wave reflection on hydraulic power. Clinical intervention with drugs that stiffen the main pulmonary artery may alleviate this problem. This approach may be of importance immediately after massive pulmonary thromboembolism when the patient is at risk of succumbing from acute right ventricular failure.

Appendix 1
Mathematical Model of Canine Pulmonary Circulation

The model of the pulmonary vasculature that we developed was similar to a model developed by others (12, 13). The properties of the main pulmonary artery were based on our own estimates of vessel length (2.4 cm) and diameter (1.38 cm) at zero transmural pressure, which corresponds to a diameter of 1.6 cm at a normal transmural pressure of 25 cm H_2O. Compliance per unit length (C_L) was estimated from these dimensions and values of wave speed. We chose a value for the inviscid fluid wave speed (C_o) of 2.6 $m \cdot s^{-1}$, which is similar to values of apparent wave speed at high frequencies in the dog of 2.55 $m \cdot s^{-1}$ (29) and 2.75 $m \cdot s^{-1}$ (30).

The determination of compliance from vascular dimensions and wave speed is based on the telegraph line equations in which the propagation coefficient (γ) is expressed in terms of the longitudinal (Z_L) and transverse (Z_T) impedance (see reference 9 for derivation).

$$\gamma = [(R_L + j\omega L_L)j\omega C_L]^{1/2} \quad (A1)$$

where ω is the angular frequency, R_L is resistance per unit length, L_L is inertance per unit length, and C_L is compliance per unit length. At high frequencies, R_L is small relative to L_L and C_L because ω is high. Therefore, the vessel wall behaves as if it were inviscid, and equation A1 can be expressed as

$$\gamma_o = j\omega[L_L C_L]^{1/2} \quad (A2)$$

where γ_o is the inviscid propagation coefficient. At high frequencies γ_o is equal to $j\omega/C_o$ (12). Inertance per unit length is estimated by $4\rho/(\pi D^2)$ where D is the diameter of the vessel and ρ is the density of blood (1.06 $g \cdot cm^{-3}$). By substituting for γ_o and L_L and rearranging, equation A2 becomes

$$C_L = (\pi D^2)/(4\rho C_o^2) \quad (A3)$$

After establishing the anatomy and compliance of the main pulmonary artery, the remainder of the pulmonary vasculature was obtained from generating coefficients. These coefficients are similar to those of Milnor, but were adjusted so that the mathematical model produced a mean Ppa and pulmonary arterial compliance similar to that measured under control conditions. The coefficients were used to generate the properties of each order of the pulmonary vasculature through to the pulmonary vein. Generation 23 is pulmonary capillaries (n = 983,040,000), D_O = 7.7 μm, and length (x) = 1.8 μm. The diameters were assumed to be the diameter at zero transmural pressure (D_O). Because of the dependence of diameter on pressure, the wave speed is a function of pressure. After

estimating the dimensions and compliance per unit length for each generation, the pressure-diameter relation (dD/dP) was calculated from the following expression:

$$dD/dP = 2C_L/(\pi D) \qquad (A4)$$

By assuming a left atrial pressure of 4 cm H_2O and specifying a value for total pulmonary blood flow ($\dot{Q}$), we estimated the intravascular pressure at each generation using the fifth power law using the expression (14):

$$[D_O + (dD/dP)P_{entry}]^5 - [D_O + dD/dP\ P_{exit}]^5 = 640\ \mu(dD/dP)x\dot{Q}/\pi \qquad (A5)$$

where μ is apparent blood viscosity and P_{entry} and P_{exit} are the entry and exit transmural pressures. The transmural pressure is the difference between the intravascular and extravascular pressure. The extravascular pressure is pleural pressure (0 cm H_2O) except for vessels with diameters less than 100 μm where alveolar pressure is the extravascular pressure; x is the length of each generation.

Characteristic impedance of the main pulmonary artery was calculated from the telegraph equations (4).

$$Z_c = [Z_L/Z_T]^{1/2} = [(R_L + j\omega L_L)j\omega C_L]^{1/2} \qquad (A6)$$

At high frequencies, R_L becomes negligible relative to $j\omega L_L$ and $j\omega C_L$; therefore, Z_c becomes equal to $[L_L/C_L]^{1/2}$ (equation 4). By rearranging equation 4 in terms of diameter instead of radius and cross-sectional area, we obtained the following expression:

$$Z_c = [8\rho(\pi^2 D_i^3\ (dD/dP)_i)]^{1/2} \qquad (A7)$$

where $(dD/dP)_i$ is the slope of the pressure-diameter relation for a particular generation number i, and D_i is the corresponding diameter at the intravascular pressure for that generation. Total arterial compliance (C_a) is estimated from the expression:

$$C_a = \sum_{i=1}^{i=22} n_i x_i\ (dD/dP)_i \cdot \pi \cdot D_i/2 \qquad (A8)$$

where i is the generation number, n_i, x_i, and D_i are the number of branches, the length, and mean diameter of a particular order of the pulmonary vasculature, denoted by subscript i.

Because the experiments were conducted with open-chested dogs, pleural pressure is always zero. The input parameters for the model are alveolar pressure and $\dot{Q}$. To simulate the snare, the number of branches downstream from Generation 1 was reduced by 50%. To simulate pulmonary embolism, the number of branches above Generation 7 was reduced by 50%.

Appendix 2
Comparison of Methods for Calculating Characteristic Impedance

In this report we used a lumped parameter model to calculate Z_c (9). Other investigators average the moduli of the impedance spectrum at high frequencies. We compared these methods by analyzing a subset of our result. We selected two impedance spectrum before and during ensnarement of the left main pulmonary artery in each of the eight experiments of the first series. Characteristic impedance was calculated by five other methods (11–15). Kendall's concordance coefficient (31) was significant ($p < 0.001$), but it was of low value: 0.56. Comparison of Spearman's rank correlation coefficients (table A1) indicates that the correlation with Z_c is significant in all cases except the last two methods. Only the last method resulted in a probability that there was no clear significant difference between characteristic impedance with ensnarement. These results indicate that the increase of characteristic impedance is not due to our method of calculating Z_c with the lumped parameter model.

TABLE A1

COMPARISON OF METHODS TO CALCULATE CHARACTERISTIC IMPEDANCE*

Method (*reference*)	Correlation with Z_c	p Value	Before SN	During SN	p Value
Present report	–	–	0.147 + 0.028 − 0.024	0.190 + 0.038 − 0.031	0.041
2 to 12 Hz (11)	0.78	0.003	0.139 + 0.027 − 0.023	0.211 + 0.052 − 0.041	0.071
3.5 to 10 Hz (12)	0.76	0.003	0.151 + 0.027 − 0.023	0.220 + 0.054 − 0.044	0.054
1 to 9 harmonics (13)	0.69	0.008	0.156 + 0.018 − 0.016	0.217 + 0.043 − 0.036	0.007
15 to 25 Hz (14)	0.05	0.846	0.163 + 0.025 − 0.022	0.213 + 0.046 − 0.038	0.052
6 to 8 harmonics (15)	0.16	0.531	0.148 + 0.033 − 0.027	0.180 + 0.059 − 0.044	0.232

Definition of abbreviations: SN = ensnarement of the left main pulmonary artery; Z_c = characteristic impedance.

* Method indicates the range of moduli that were averaged to estimate characteristic impedance (Z_c). Spearman rank correlation coefficients (31) were used to compare Z_c measured by the lumped parameter model with Z_c measured by five other methods that are based on averaging the moduli of the impedance spectrum at selected frequencies. Characteristic impedance values before and during ensnarement were compared with log normal transformation of the data, mean values ± 1 SEM are given as 10^3 dyn·cm^{-5}·s.

Acknowledgment

The writers thank Dr. W. R. Milnor for his assistance during the development of the mathematical model, Janssen Pharmaceutica for donating a supply of ketanserin, C. Theophilos and A. Wurtenberger for technical assistance, M. Barber and B. Sauka for secretarial assistance, and Dr. R. A. Klocke for reviewing the manuscript.

References

1. Moser K. Pulmonary embolism. Am Rev Respir Dis 1977; 115:829–51.
2. Milnor WR. Arterial impedance as ventricular afterload. Circ Res 1975; 36:565–70.
3. Milnor WR, Bergel DH, Bargainer JD. Hydraulic power associated with pulmonary blood flow and its relation to heart rate. Circ Res 1966; 19: 467–80.
4. Grant BJB, Paradowski LJ. Characterization of pulmonary arterial input impedance with lumped parameter models. Am J Physiol 1987; 252:H585–93.
5. Westerhof G, Van den Bos C, Laxminarayan S. Arterial reflection. In: Bauer RD, ed. Arterial system. Berlin: Springer-Verlag, 1975; 48–62.
6. Fung YC. Biodynamics: circulation. New York: Springer-Verlag, 1984; 121.
7. Wiener F, Morkin E, Skalak R, Fishman AP. Wave propagation in the pulmonary circulation. Circ Res 1966; 19:834–50.
8. Milnor WR. Hemodynamics. Baltimore: Williams and Wilkins 1982; 338–40.
9. Zhuang FY, Fung YC, Yen RT. Analysis of blood flow in cat's lung with detailed anatomical and elasticity data. J Appl Physiol 1983; 55:1341–8.
10. Snedecor GW, Cochran WG. Statistical methods. 7th ed. Ames: Iowa State University Press, 1980; 255–333.
11. Elkins RC, Milnor WR. Pulmonary vascular response to exercise in the dog. Circ Res 1971; 29:591–9.
12. O'Rourke MF, Taylor MG. Input impedance of the systemic circulation. Circ Res 1967; 20:365–80.
13. Westerhof N, Elzinga G, Van der Bos GC. Influence of central and peripheral changes on the hydraulic input impedance of the systemic arterial tree. Med Biol Eng 1973; 710–23.
14. Peluso F, Topham WS, Noordergraaf A. Response of systemic input impedance to exercise and graded aortic constriction. In: Baan J, Noordergraaf A, Raines J, eds. Cardiovascular system dynamics. Cambridge: MIT Press, 1978; 432–40.
15. Abel FL. Fourier analysis of left ventricular performance. Evaluation of impedance matching. Circ Res 1971; 28:119–35.
16. Comroe JH, Van Lingen B, Stroud RC, Roncoroni A. Reflex and direct cardiopulmonary effects of 5-OH-tryptamine (serotonin): their possible role in pulmonary embolism and coronary thrombosis. Am J Physiol 1953; 173:379.
17. Huet Y, Brun-Buisson C, Lemaire F, Teisseire B, Lhoste F, Rapin M. Cardiopulmonary effects of ketanserin infusion in human pulmonary embolism. Am Rev Respir Dis 1987; 135:114–7.
18. Utsunomiya T, Krausz MM, Levine L, Shepro D, Hechtman HB. Thromboxane mediation of cardiopulmonary effects of embolism. J Clin In-

vest 1982; 70:361–8.
19. Coleridge JCG, Kidd C. Electrophysiological evidence of baroreceptors in the pulmonary artery of the dog. J Physiol (Lond) 1960; 150:319–31.
20. Fozard JR. Mechanism of the hypotensive effect of ketanserin. J Cardiovasc Pharmacol 1982; 4:829–38.
21. Segal SS, Duling BR. Communication between feed arteries and microvessels in hamster striated muscle: segmental vascular responses are functionally coordinated. Circ Res 1986; 59:283–90.
22. Verbeuren TJ, Jordaens FH, Hermen AG. Accumulation and release of [^{3}H]-5-hydroxytryptamine in saphenous veins and cerebral arteries of the dog. J Pharmacol Exp Ther 1983; 226:579–88.
23. Van den Bos GC, Westerhof N, Randall OS. Pulse wave reflection: can it explain the differences between systemic and pulmonary pressure and flow waves? A study in dogs. Circ Res 1982; 51:479–85.
24. Bergel DH, Milnor WR. Pulmonary vascular impedance in the dog. Circ Res 1965; 16:401–15.
25. Calvin JE Jr, Baer RW, Glantz SA. Pulmonary artery constriction produces a greater right ventricular dynamic afterload than lung microvascular injury in the open chest dog. Circ Res 1985; 56:40–56.
26. Pouleur H, LeFeure J, van Eyll C, Jaumin PM, Charlier RA. Significance of pulmonary input impedance in right ventricular performance. Cardiovasc Res 1978; 12:617–29.
27. Aramendia P, Taguini CM, Fourcade A, Taguini AC. Reflex vasomotor activity during unilateral occlusion of the pulmonary artery. Am Heart J 1963; 66:53–60.
28. Guyton AC, Lindsey AW, Gilluly J. The limits of right ventricular compensation following acute increase in pulmonary circulatory resistance. Circ Res 1954; 11:326–32.
29. Attinger EO. Pressure transmission in pulmonary arteries related to frequency and geometry. Circ Res 1963;12:623–41.
30. Bargainer JD. Pulse wave velocity in pulmonary artery of the dog. Circ Res 1967; 20:630–7.
31. Siegel S. Nonparametric statistics for behavioral sciences. Tokyo: McGraw-Hill Kogkusha. 1956; 195–239.